Landmine detection in hyperspectral images based on pixel intensity

Landmine Detection in Hyperspectral Images based on Pixel Intensity

Mahdi Khodor[a,b,1], Ihab Makki[c], Rafic Younes[a], Tiziano Bianchi[b], Jihan Khoder[a], Clovis Francis[a], Massimo Zucchetti[b]

[a] Faculty of Engineering Lebanese University Badaro, Museum, 65730, Beirut, Lebanon
[b] Politecnico di Torino, Corso Duca Abruzzi, 24, 10129, Torino, Italy
[c] International University of Beirut, Mouseitbeh, 14640, Beirut, Lebanon

Abstract. Hyperspectral imaging is a technique used to collect the same scene with different wavelengths, achieving both high spectral and spatial resolution. Hyperspectral imaging plays an important role in several scenarios involving target detection, among which landmine detection is a very challenging one. In this work, we developed a procedure based on pixel similarity measures to detect rare pixels present in a scene. The method can be combined with most of the existing detection algorithms in order to reduce the complexity and improve the performance. The developed method was tested on various types of hyperspectral images where the spectra of the landmines were simulated in different parts of the scenes with different mixing factors. The performance of the proposed method is also confirmed by tests made in real scenarios. Comparisons with state-of-the-art existing algorithms demonstrate that the method achieves excellent detection performance, with a reasonable computational complexity.

Keywords: Hyperspectral Imaging, Pixel Similarity Methods, landmine detection, Remote Sensing, Dimensionality Reduction.

1 Introduction

Third world countries have long suffered from the problem of landmines that threaten citizens (Zucchetti et al. 2017; UNICEF., Children, and Conflict 2009). This problem damages the development of social and economic regions, for example affecting cultivated areas (Hulme 2009). Currently, more than 110 million mines are present in 70 countries (MacDonald et al. 2003). The manufacturing cost does not exceed $3 per mine, but the demining costs are about $1100 per mine (MacDonald et al. 2003). In 2017, the Landmine Monitor recorded 7239 casualties by landmines, 2793 people were killed, 4431 people were injured (Makki et al. 2017; Monitor, Policy, and Action 2010; Makki et al. 2018; Zucchetti et al. 2017). Different techniques have been used in order to detect landmines. Each of these methods have its advantages and inconveniences. The most used

[1] Address all correspondence to Mahdi Khodor, E-mail: mahdi.khodor@polito.it

methods are electromagnetic methods (MacDonald et al. 2003), Ground Penetrating Radar (GPR; MacDonald et al. 2003; Kale, Ratnaparkhe, and Bhalchandra 2013) Acoustic/Seismic method (Mukhopadhyay and Gupta 2007), Nuclear Quadruple Resonance (NQR; Robledo, Carrasco, and Mery 2009). These methods are dangerous because they require the presence of demining units in the minefield, or like the metal detector suffer from high false alarm rate caused by tiny amount of metals (Cardona, Jiménez, and Vanegas 2014). For these reasons, we are searching for a new solution that can be safer and faster based on hyperspectral imaging.

1.1 State of the art

In the literature, we found different algorithms used for target detection using hyperspectral images (Manolakis and Shaw 2002; Zou and Hastie 2005). Generally, we can classify those algorithms in two types: supervised algorithms where we search for a known spectrum that characterizes the target; unsupervised algorithms, known as anomaly detectors, where pixels different from their surrounding are marked as targets. The latter type could be used in a preliminary stage to reduce the working area before identifying the target using a supervised method. In this paper, we will use some rare event detectors in the first step to detect the suspected pixels and then apply in the second step a target detection algorithm. We are considering different cases of full-pixel and subpixel targets.

Numerous algorithms were proposed for target detection in hyperspectral imaging. Even if target detection in Hyperspectral images is not limited to the following algorithms, these algorithms are the most commonly used ones: Adaptive Coherence Estimation (ACE; Scharf and McWhorter 1996), Matched Filter (MF; Manolakis et al. 2013), Constrained Energy Minimization (CEM; Ren et al. 2003), Multiple target CEM (MTCEM; Ren et al. 2003), Winner take all CEM (WTACEM),

Orthogonal Subspace Projection (OSP; Harsanyi and Chang 1994), Spectral Angular Mapper (SAM; Wang and Zhao 2016), Spectral Information Divergence (SID; Chang 1999).

These algorithms do not support the detection of several targets at the same time. So, the algorithm should be applied several times, each run searching for a specific target. But this will be a time-consuming process especially if the number of targets is high. Few algorithms have been extended to the multitarget case, like CEM. This algorithm is able to estimate the abundance of a target in a hyperspectral image. Many algorithms are extended from CEM e.g. MultiCEM, SumCEM, WTACEM and others (Yin et al. 2010).

The amount of data captured with hyperspectral imaging is very large (August et al. 2013). Moreover, the processing of this amount of data can be very complex and time consuming. Therefore, the need for dimensionality reduction in hyperspectral imaging motivated many researches in this field. Since in hyperspectral imaging neighboring bands appear similar and may contain the same information (Guo et al. 2008) many researchers have proposed dimensionality reduction using band selection methods (Chen, Jiang, and Yoshihira 2006; Guo et al. 2006; Du and Yang 2008). Some of these methods are supervised and some of them are unsupervised. Many of the methods do not preserve rare objects after reduction, while some of them do not preserve the local/global geometric structure on reduced data volumes. In the following, we consider two methods based on band selection that preserve rare objects after reduction: Multicriteria classification method (Khoder et al. 2017) and the Net Analyte signal method (NAS; Grahn and Geladi 2007).

1.2 Our contribution

Some of the existing algorithms are characterized by a high false alarm rate during target detection and some of them have high computational complexity (Camacho Velasco, Vargas García, and Arguello Fuentes 2016). To solve these problems, in this paper we propose a technique based on anomaly detection.

We detect anomalies using a pixel intensity similarity measured at the pixel level in order to reduce the number of pixels, before applying the best performing detection algorithm. In addition, we study the ability to reduce the size of the hypercube at the band level by using two dimensionality reduction methods based on band selection in order to retrieve the most representative bands to detect all the types of landmines, and we evaluate the performance of each method by evaluating detection performance and false alarm rate after reduction.

1.3 Organization

This article is organized as follows: in Section 2, the proposed methodology is presented. The experimental setting and the adopted criteria are shown in Section 3. In Section 4 we discuss the results of the best performing classification algorithm and the pixels intensity method when applied on AVIRIS hyperspectral images in which we simulate landmines using real landmine signatures. We also compare the performance of two band selection methods in order to verify the ability of reducing the number of image bands without losing performance in target detection. The best performing algorithm is finally tested on a realistic hyperspectral image taken in the lab. Conclusions and future research directions are drawn in Section 5.

2 Proposed Methodology

In this section, we first introduce the main idea of the developed procedure, then we give a detailed description of each step. First, we use Pixel Intensity (PI) method at the pixel level to detect objects that appear rarely in the images.

If PI value is greater than a certain threshold, we decide that the pixel is rare, and we save it. This strategy is repeated for all pixels in all the bands. After storing all the rare pixels, we obtain a new data structure containing only the rare pixels in the original hyperspectral image, thus decreasing the image size.

In order to discriminate the rare objects resulting from the previous step, we apply one of the existing detection methods in hyperspectral imaging, which are described in the next section. This will decrease the complexity of the existing detection methods and, in some cases, may improve their performance in terms of false alarm and detection probability.

2.1 Pixel Intensity Method

Some rare objects or targets appear only in a limited number of bands (Yu, Song, and Chang 2018; Guo, Pu, and Cheng 2016). Therefore, we choose to analyze each pixel value in each band instead of the average value of a pixel in all bands, in order to be able to detect the presence of rare events even in few bands. When considering the average value of a pixel in all bands, small rare objects having a small difference with respect to their neighbors can be difficult to detect. Also, experimental results confirm that working on a single pixel value for each band performs better than the average value in terms of detection of rare objects.

We can define an anomaly or a rare event as an object in the scene that differs in a substantial way from the surrounding objects, as shown in Fig. 1. (Khoder and Younes 2013; Khoder et al. 2015).

Figure 1. Image Containing a Rare Event.

PI represents the amount of gray level in the pixel, i.e., its brightness (Kumar and Verma 2010). Using this method, we compute how much the intensity of a pixel is different from that of surrounding pixels. Also, PI is the square root of the squared error criterion (Wang et al. 2004). The equation is given by:

$$PI = \left|(a_i - \bar{\mu})\right| \quad (1)$$

Where a_i is the pixel value and $\bar{\mu}$ is the average of the pixel values in a neighborhood of a_i.

Let us consider a hyperspectral image $I(x, y, \lambda)$ having n_λ spectral bands. In the context of our algorithm we consider the following steps:

- Scan each pixel in each band.
- Compute the similarity measure between pixel and neighborhood (figure 2).
- If the similarity measure is above a certain threshold, the pixel is rare and then we store its position.
- Finally, after all bands are scanned, we get a dataset containing the rare pixels positions.

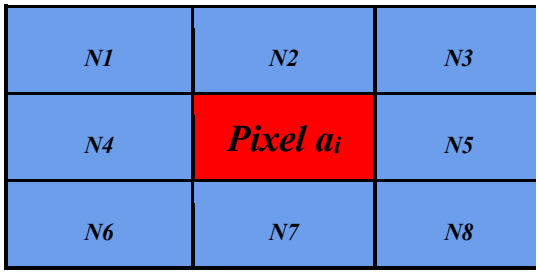

Figure 2. Representation of pixel Aij and its neighborhood Nk.

When using this neighborhood, we are assuming that the size of rare objects is just a single pixel. In our scenario this is fine because the size of a landmine usually does not exceed one pixel. However, if the resolution of images increases and targets become larger than a single pixel, we can compute the similarity considering a larger window for the target and a subsequently larger neighborhood.

The above algorithm returns only rare objects in the image, without any indication concerning the type of each target. Therefore, we apply one of the best performing existing detection algorithms to the set of rare pixels to classify them.

2.2 *Adaptive coherence estimator (ACE)*

As discussed in the background section, there are several available algorithms for target detection in hyperspectral images. Several studies demonstrate that ACE is the best performing algorithm in terms of probability of detection and false alarm rate (Camacho Velasco, Vargas García, and Arguello Fuentes 2016; Basener, Nance, and Kerekes 2011). However, ACE has a high computational cost compared to other methods. In this study, ACE method is applied after the PI method. This will reduce the complexity of ACE and may improve its performance in terms of false alarm and probability of detection.

ACE is based on the statistical approach. It is derived from the generalized maximum likelihood ratio test (Broadwater and Chellappa 2007):

The problem is posed as a hypothesis testing problem between the two hypotheses:

H0: Mine absent (Background material)
H1: Mine present

$$H_0: \boldsymbol{x} \sim N(0, \sigma_0^2 \boldsymbol{\Sigma_b}) \quad (1)$$

$$H_1: \boldsymbol{x} \sim N(a\mathbf{s}, \sigma_1{}^2 \boldsymbol{\Sigma_b})$$

Where 0 is the background mean vector, **s** is the target spectrum, $\boldsymbol{\Sigma_b}$ is the covariance matrices of background, a and σ are scaling factors. The covariance matrix of the background is estimated from the data surrounding the pixel under test. The likelihood ratio will be:

$$L(\boldsymbol{x}) = \frac{f(\boldsymbol{x}/H_1)}{f(\boldsymbol{x}/H_0)} \quad (2)$$

In practice, for evaluating the above likelihood ratio, the values of the scaling factors are replaced by their maximum likelihood estimates, which gives the following generalized likelihood ratio test known as the ACE detector:

$$y_{ACE} = \frac{\boldsymbol{x}^T \boldsymbol{\Sigma_b}^{-1} \boldsymbol{s} (\boldsymbol{s}^T \boldsymbol{\Sigma_b}^{-1} \boldsymbol{s})^{-1} \boldsymbol{s}^T \boldsymbol{\Sigma_b}^{-1} \boldsymbol{x}}{\boldsymbol{x}^T \boldsymbol{\Sigma_b}^{-1} \boldsymbol{x}} \quad (3)$$

Where **x** is a vector representing the reflectance spectrum of the pixel under test, **s** is a vector containing the signature of the target, $\boldsymbol{\Sigma_b}$ is the covariance matrix of the background.

3 Materials and Methods

3.1 Simulated landmine experiment

Our dataset consists of 17 hyperspectral image scenes acquired using AVIRIS sensor and processed as in Makki et al. (2018). The scenes are originally composed of 224 bands between 394 nm and 2500 nm with spectral resolution of 10 nm and spatial resolution of 20 m. We applied several image preprocessing steps including the elimination of water absorption bands and low pass filtering to remove the bands that have a spectral response above 1nm. We simulated in different locations of the scenes the spectral signatures of the 6 types of landmines (figure 3) shown in figure 4. These signatures were collected using an ASD field spectroradiometer. Acquisitions

were made in our laboratory using a special source of illumination. This source is specified by the 70-watt quartz-tungsten-halogen light source with integrated reflector, creating stable illumination over the 350 to 2500 nm range. The targets were simulated in different proportions using the following formula:

$$\boldsymbol{ps} = \alpha * \boldsymbol{t} + (1 - \alpha)\boldsymbol{b} \tag{4}$$

where **ps** is the simulated spectrum in the image, **t** is the target reflectance spectrum represented as a vector, **b** is the reflectance of background material and α is the abundance factor of the target, which varies between 0.1 and 0.9. Since, the spatial resolution of the AVIRIS image is much larger than the landmine size, the image is upsampled in order to increase the spatial resolution and have pixel size equivalent to the size of the mine.

Figure 3. 6 different landmines.

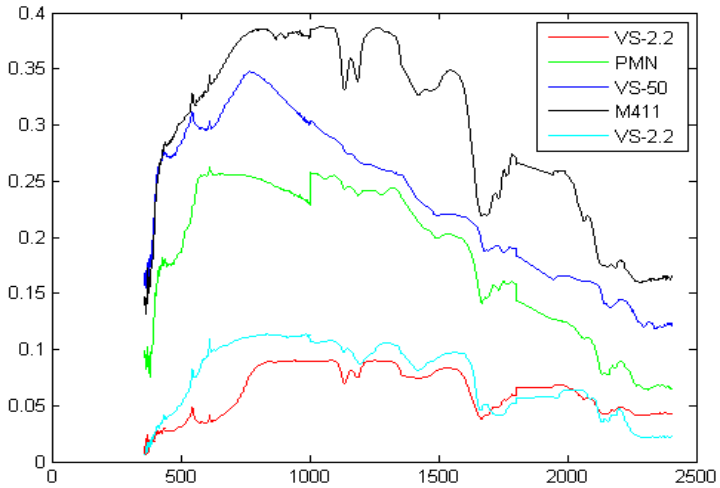

Figure 4. 6 Landmine Spectra.

Using these scenes, we tested the performance of ACE method and ACE method combined with the pixel intensity measure. We will evaluate the performance of these two algorithms based on three criteria:

Detection Rate (DR): which is the ratio between the number of detected targets and the number of targets in the scene. In the landmine scenario missing detection can be very dangerous, so the detection rate should ideally be one.

False positive rate (FPR): this is the number of false positives per unit area. This value counts the average number of non-target pixels detected as target per unit area (m^2). This value is dependent on the image size. To be more general, and to remove the effect of image resolution, we use also the **Relative False Positive Rate (RFPR)**. This value is the ratio between the number of false positives and the sum of true positives and false positives.

$$\text{FPR}=\frac{FP}{image\ resolution*(pixel\ size)^2} \quad (5)$$

$$\text{RFPR}= \left(\frac{FP}{TP+FP}\right) * 100 \quad (6)$$

True positive (TP): target pixel correctly detected as target

false positive (FP), non-target pixel wrongly detected as target

Computation time (CT): CPU time registered in seconds needed to execute the algorithms.

The measurement of the detection rate and FPR depends on the threshold chosen in the classification phase to discriminate between target and non-target pixels. When comparing different detection methods, the Receiver Operating Curve (ROC), visualizes the detection rate in terms of FPR for different choices of the threshold. However, in our scenario, due to the low presence of targets, ROC curve is not the ideal method of evaluating the detection performance. Since in our scenario missing a target can be very dangerous, the threshold is set in such a way as to detect all targets and then the FPR is calculated. Therefore, an algorithm is more efficient if it has a lower FPR and lower computational time when all targets are detected (DR=1). It is worth noting that, since the two type of errors in hypothesis testing are dual, according to the Neyman-Pearson lemma a detector based on the likelihood ratio test is also guaranteed to minimize the probability of false alarm in this setting.

3.2 Real Landmine Experiment

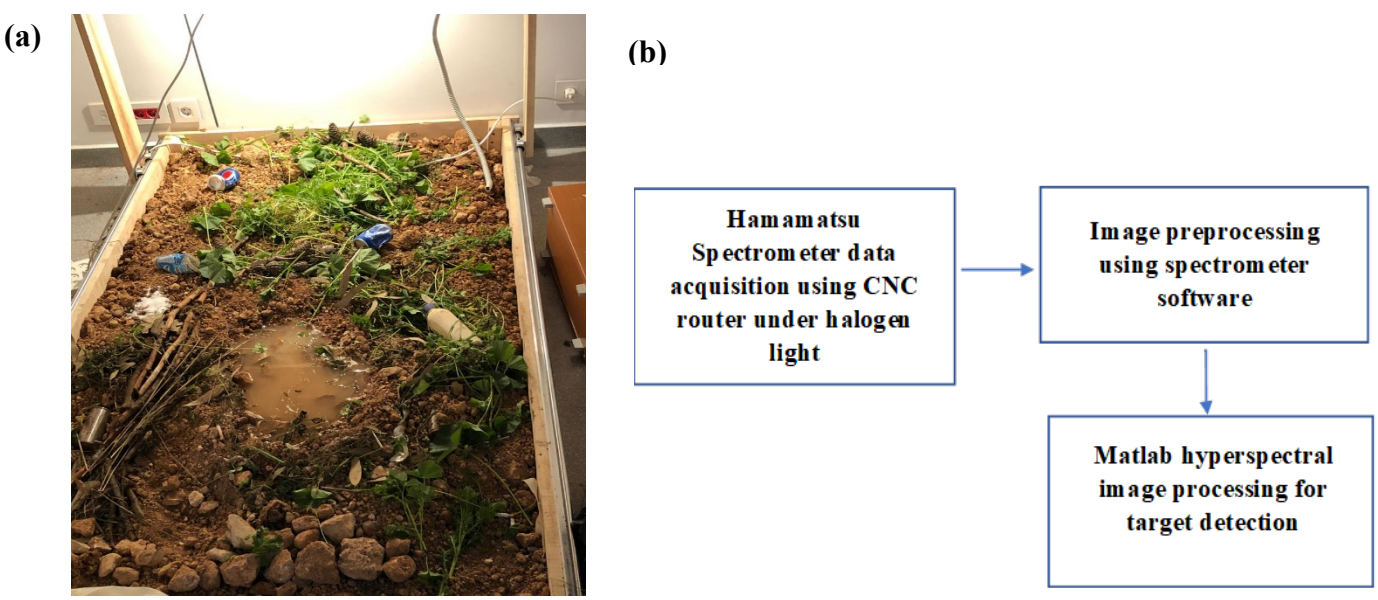

Figure 5. (a) presented scene (b) schematic figure for data acquisition and processing.

This experiment consists in a scene presented in figure 5 (a). An area containing soil, grass, wood, water, and multiple materials is prepared to be more realistic. Figure 5(b) represents the data acquisition and processing steps and materials of the experiment.

A computer numerical control (CNC) router (Jayachandraiah et al. 2014) is used to handle the spectrometer and scan the whole area. A Hamamatsu spectrometer (Shibayama 2009) is used with a spectral range between 350 and 1700 nm and a spectral resolution of 3 nm.

In the reproduced scene, 2 types of landmine are used (Figure 6): a plastic landmine and a metal landmine for a realistic simulation we used two containers with the same material as the real landmines (the metal landmine represents the cluster bomb and the plastic one represents the vs50 landmine). In addition, the same explosive powder is used in the two types of landmines. This powder is a type of TNT explosive with nitrating mixture (conc. sulfuric & conc. nitric acid).

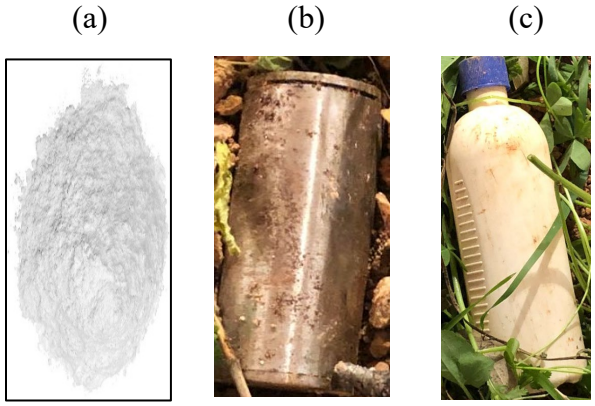

Figure 6. (a) explosive powder. (b)metal landmine. (c) plastic landmine.

Figure 7 shows some landmine distribution cases, where landmines are deployed in different positions in order to mimic a realistic scenario. Using the explosive powder is important in our experience because in most cases, when the landmines stay a long time in the area, the powder material may seep from landmines.

Figure 7. Landmines distribution scenarios.

4 Results and discussion

4.1 Comparative study between ACE and PI+ACE

In this part, we show the results obtained when applying the two used methods on all images that contain targets with different abundances. We show the average false alarm rate and computation time at full target detection rate. The experiments were carried out in MATLAB environment under Intel operator (TM) 6276 with 64 CPU and 2.9 GHz processor frequency with 128 GB RAM. Comparisons are made between PI+ACE and ACE in the two experimental settings previously described.

4.2 Simulated landmine experiment

As discussed above, the decision threshold used to detect rare pixels and the other thresholds to identify the landmine types for the existing detection techniques are set to be the lowest value such that all targets are detected (DR=1) and then the FPR is registered. Therefore, a technique is said to be more efficient if it has lower FPR when all targets have been detected. In order to set the threshold, we use a dataset of 5 images for training and we use the remaining 12 images for testing. For each landmine abundance factor, we compute a different threshold. Hence, we measure DR and FPR on the testing dataset using the same threshold.

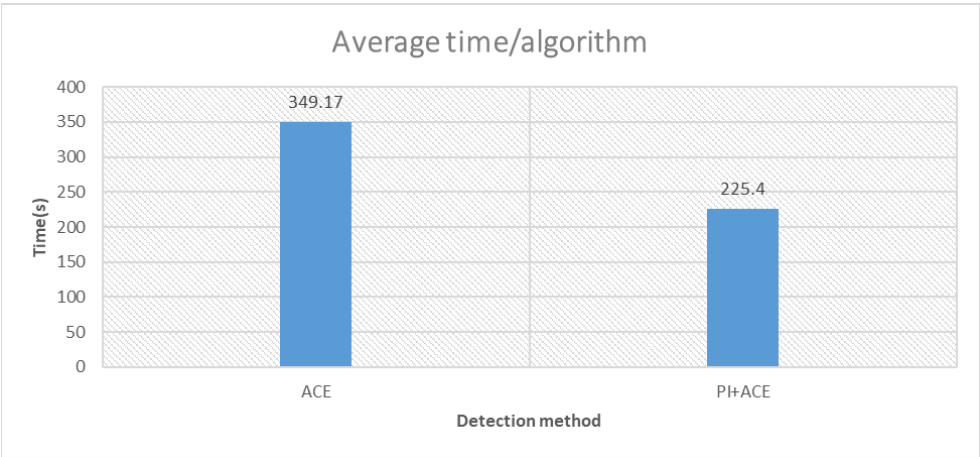

Figure 8. Average computational time /algorithm.

In Figure 8, the average time needed by each algorithm to detect all the targets in the 12 images is shown. As we see in the Figure 8, to detect both types of targets using ACE we needed about 349.17 seconds while the computation time of PI+ACE is 225.4 seconds.

Table1 . Average DR for each mine with 0.9-0.1 abundance factor.

Algorithm/target	PMN	VS-2.2	VS-50	N°4	M411	TM-46
ACE	1	0.9975	1	1	1	1

PI+ACE	1	1	1	1	1	**1**

Table 2. Average FPR/m2 and RFPR for each mine with 0.9-0.1 abundance factor.

Target	**PMN**	**VS-2.2**	**VS-50**	**N°4**	**M411**	**TM-46**
Algorithm	**ACE**					
FPR	0.00001	0.58790	0	0	0.4300	0
RFPR	0.00122%	72.25%	0	0	58.2%	0
Algorithm	**PI+ACE**					
FPR	0	0.00032	0	0	0.00058	0
RFPR	0	0.04%	0	0	0.0077%	0

In Tables 1 and 2 we show the detection performance of two tested algorithms, when the landmine abundance factor is between 0.9 and 0.1. As we see in Table 2, using the similarity measures before ACE, we can decrease the FPR from 0.58 and 0.43 to 0.00032 and 0.000058 in case of VS-2.2 and M411 mines, respectively. Similar results can be observed for RFPR. In the other types of mines, we measure 0 FPR when applying similarity measures before ACE, indicating that in these cases we expect the FPR to be less than 1/number of tested pixels. Overall, PI+ACE method has the lowest FPR with the lowest CT compared to ACE with DR=1. It is important to note that some targets have 0 FPR while other targets have high FPR. This is due to the material of each target and their spectral similarity with the background pixels.

Concerning the detection rate, ACE has DR or less than one concerning the VS-2.2 landmines where it can detect all the other types of landmines with DR=1. When we apply the similarity methods before ACE, we get DR=1 in all the types of landmines.

4.3 Real landmine experiment

Figure 9 shows the RGB representation of the scene acquired in the lab. The spatial resolution is $0.16m^2$. The size of obtained image is 25*40 pixels.

Figure 9. RGB representation of real scene.

Table 3 show the results of FPR and RFPR in the two cases when ACE is used and when PI+ACE is used. All the results in this table is with DR=1.

Table 3. Average FPR/m2 and RFPR for each mine.

target	**Metal Landmine**	**Plastic Landmine**	**Powder**
Algorithm	**ACE**		
FPR	0.009	0.013	0
RFPR	12.33%	18.1%	0
Algorithm	**PI+ACE**		
FPR	0	0	0
RFPR	0%	0%	0%

From table 3, we can observe that when we use PI+ACE both FPR and RFPR decrease for the two types of landmines and we are not able to measure any false positive. It is important to clarify that in this experiment we cannot measure any significant FPR less than 1/1000, since the tested image has a size of 1000 pixels.

4.4 Band Selection

After verifying that PI+ACE method has the best performance concerning FPR, CT and DR, here we study the effect of net analyte signal (NAS) and multicriteria band selection methods on the performance of PI+ACE method.

NAS is defined as the part of an analyte spectrum that is singular to that analyte (Lorber 1986). This method is supervised, takes the spectrum of the target and the image as input, and returns the bands that represent the selected target.

Multicriteria method is an unsupervised method. It works on classifying the set of neighboring bands based on three criteria: Mutual Information (MI), fidelity, and the cross-correlation coefficient. If these three criteria between two successive bands are above a certain threshold at the same time, these two bands are classified in the same class: this procedure is repeated for all the bands. After classifying bands; the more informative (highest entropy) band is selected from its class (Khoder 2013; Khoder et al. 2017).

We apply these two methods before applying PI+ACE. First, we apply the NAS method to visualize the representative bands for each landmine and determine the optimal range for the detection of all landmine types. Second, the multicriteria method is applied in order to obtain the most representative bands in the images. Therefore, we visualize how much we can reduce the image size without affecting the performance of PI+ACE: Figure 10 shows the FPR increase as a

function of the reduction rate, considering the two reduction methods, on the simulated landmine dataset.

Table 4 shows the optimal bands for each type of landmine of the simulated landmine dataset. To cover all the types of landmines we need a spectral range between 900 nm and 2500 nm.

When multicriteria is used we obtain that the optimal range to detect all the landmines types is between 1100 nm and 2250 nm. The advantages of multicriteria over the NAS method is that we can reduce the image size based on whatever the types of targets present in the image are, achieving higher reduction rates.

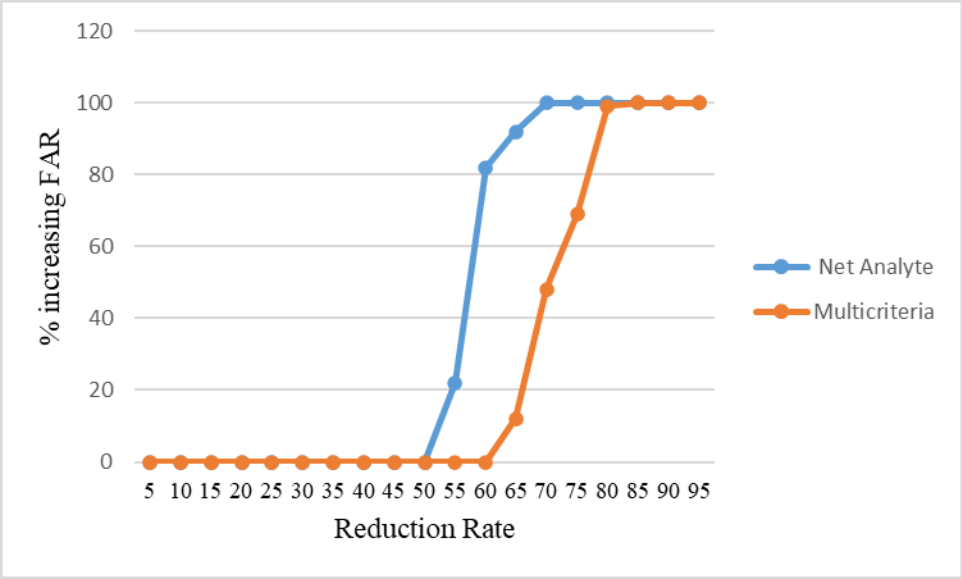

Figure 10. FAR increase (%) of PI+ACE as a function of reduction rate.

Table 4. Optimal range for each landmine for the NAS signal method.

landmine	Optimal Range
Vs22:	909 nm to 1432 nm
PMN	685 nmto 1005 nm
N4	909 nm to 1177 nm

TM46	**1629 nm to 2097 nm**
M411	**928 nm to 1502 nm**
Vs50	**909 nm to 1337 nm**
All types	**900 nm 2500 nm**

Without affecting the performance of PI+ACE we can reduce the images up to 52% using the NAS method and up to 60% using the multicriteria method.

Using NAS method, Table 5 displays the main range for each landmine type in the real landmine case. As can be seen, the most informative frequency range for all the landmines types is between 380 and 1700 nm. When multicriteria is applied the selected bands are between 911 and 1700 nm.

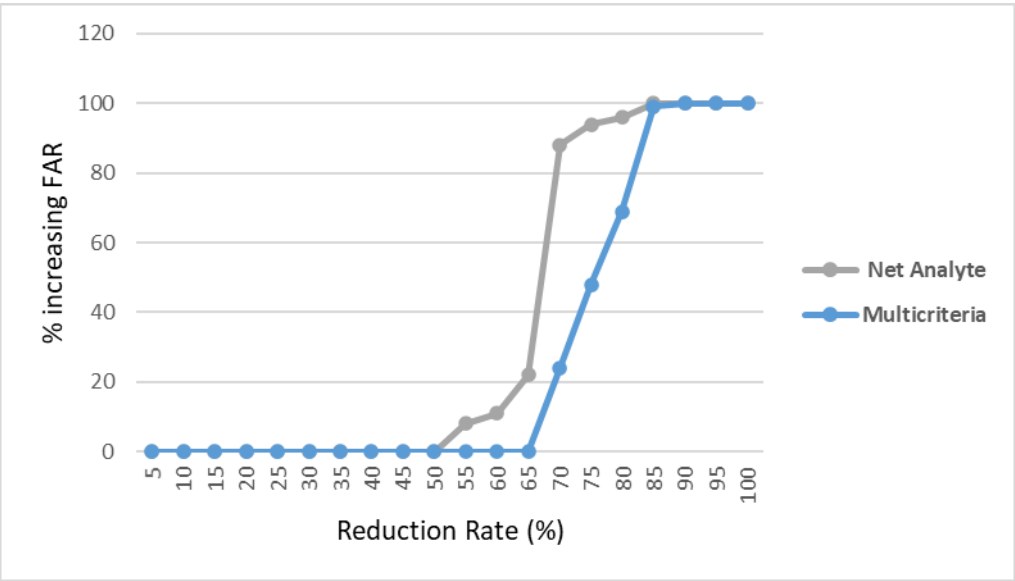

Figure 11. % of increasing of FAR of PI+ACE after reduction.

Figure 11 shows the FPR increase as a function of the reduction rate on the real landmine image. Using NAS method we can reduce the image up to 52% whereas using the multicriteria method we can reduce the image up to 66%.

Table 5. Optimal range for each landmine for the NAS signal method

landmine	Optimal Range
Metal	600 to 1700 nm
Plastic	380 to 1350nm
Powder	411 to 1120nm
All types	380 to 1700nm

Concerning the execution time figure 12 shows the execution time of PI+ACE after maintaining the two bands selection methods.

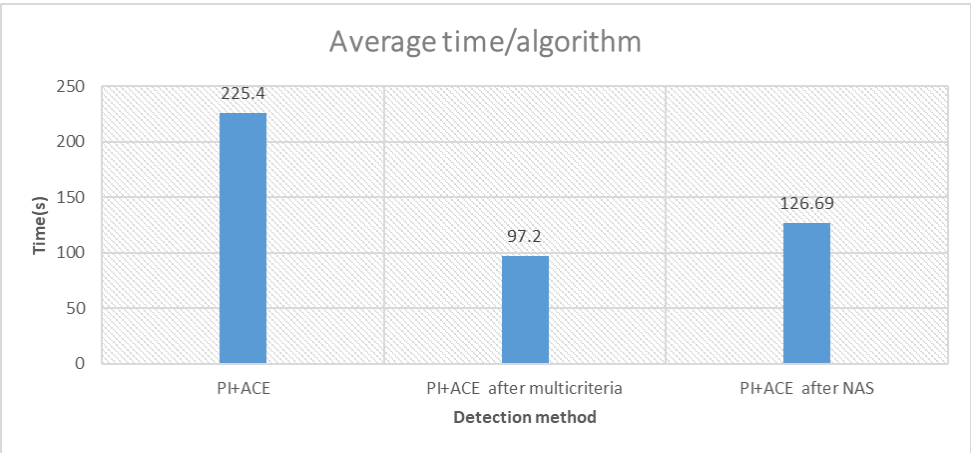

Figure 12. Execution time of PI+ACE after the two bands selection methods.

5 Conclusions

In this paper, we proposed a pixel similarity method to improve landmine detection in hyperspectral images. The rationale is to select only highly dissimilar pixels as potential targets, before applying a state of the art target detection algorithm.

Results obtained on simulated images and realistic images demonstrate that by using the pixel similarity methods with ACE, we can reduce both the execution time of ACE and reduce false alarm at 100% detection rate.

In addition, two dimensionality reduction methods based on band selection are used before applying PI+ACE method: NAS and multicriteria. We can have up to a 60 % reduction of the image without losing the performance of detection method (PI+ACE). The execution time of ACE also decreases by about 60%. Moreover, using pixel similarity after the band selection method, we can simultaneously decrease the image at the band and pixel levels without affecting the performance.

Acknowledgment

This research was supported by a grant from Erasmus+ programme http://dx.doi.org/10.13039/501100010790.

6 References

August, Yitzhak, Chaim Vachman, Yair Rivenson, and Adrian Stern. 2013. 'Compressive hyperspectral imaging by random separable projections in both the spatial and the spectral domains', *Applied optics*, 52: D46-D54.

Basener, William F, Eric Nance, and John Kerekes. 2011. "The target implant method for predicting target difficulty and detector performance in hyperspectral imagery." In *Algorithms and Technologies for Multispectral, Hyperspectral, and Ultraspectral Imagery XVII*, 80481H. International Society for Optics and Photonics.

Broadwater, Joshua, and Rama Chellappa. 2007. 'Hybrid detectors for subpixel targets', *IEEE transactions on pattern analysis and machine intelligence*, 29: 1891-903.

Camacho Velasco, Ariolfo, César Augusto Vargas García, and Henry Arguello Fuentes. 2016. 'A comparative study of target detection algorithms in hyperspectral imagery applied to agricultural crops in Colombia', *Tecnura*, 20: 86-99.

Cardona, Lorena, Jovani Jiménez, and Nelson Vanegas. 2014. 'Landmine detection technologies to face the demining problem in Antioquia', *Dyna*, 81: 115-25.

Chang, Chein-I. 1999. "Spectral information divergence for hyperspectral image analysis." In *IEEE 1999 International Geoscience and Remote Sensing Symposium. IGARSS'99 (Cat. No. 99CH36293)*, 509-11. IEEE.

Chen, Haifeng, Guofei Jiang, and Kenji Yoshihira. 2006. "Robust nonlinear dimensionality reduction for manifold learning." In *18th International Conference on Pattern Recognition (ICPR'06)*, 447-50. IEEE.

Du, Qian, and He Yang. 2008. 'Similarity-Based Unsupervised Band Selection for Hyperspectral Image Analysis', *IEEE Geosci. Remote Sensing Lett.*, 5: 564-68.

Grahn, Hans, and Paul Geladi. 2007. *Techniques and applications of hyperspectral image analysis* (John Wiley & Sons).

Guo, Baofeng, Robert Damper, Steve Gunn, and James Nelson. 2008. 'A fast separability-based feature-selection method for high-dimensional remotely sensed image classification', *Pattern Recognition*, 41: 1653-62.

Guo, Baofeng, Steve R Gunn, Robert I Damper, and James DB Nelson. 2006. 'Band selection for hyperspectral image classification using mutual information', *IEEE Geoscience and Remote Sensing Letters*, 3: 522-26.

Guo, Qiandong, Ruiliang Pu, and Jun Cheng. 2016. 'Anomaly detection from hyperspectral remote sensing imagery', *Geosciences*, 6: 56.

Harsanyi, Joseph C, and C-I Chang. 1994. 'Hyperspectral image classification and dimensionality reduction: An orthogonal subspace projection approach', *IEEE Transactions on geoscience and remote sensing*, 32: 779-85.

Hulme, Karen. 2009. 'III. The 2008 cluster munitions convention: Stepping outside the CCW framework (again)', *International & Comparative Law Quarterly*, 58: 219-27.

Jayachandraiah, B, O Vamsi Krishna, P Abdullah Khan, and R Ananda Reddy. 2014. 'Fabrication of low cost 3-Axis CNC router', *International Journal of Engineering Science Invention*, 3: 1-10.

Kale, MG, VR Ratnaparkhe, and AS Bhalchandra. 2013. 'Sensors for landmine detection and techniques: A review', *International Journal of Engineering Research and Technology*, 2: 1-7.

Khoder, Jihan. 2013. 'Nouvel algorithme pour la réduction de la dimensionnalité en imagerie hyperspectrale'.

Khoder, Jihan, and Rafic Younes. 2013. "Proposal for preservation criteria to rare event. Application on multispectral/hyperspectral images." In *2013 25th International Conference on Microelectronics (ICM)*, 1-4. IEEE.

Khoder, Jihan, Rafic Younes, Hussein Obeid, and Mohamad Khalil. 2015. "Dimension reduction of hyperspectral image with rare event preserving." In *Iberian Conference on Pattern Recognition and Image Analysis*, 621-29. Springer.

Khoder, Mahdi, Serge Kashana, Jihan Khoder, and Rafic Younes. 2017. 'Multicriteria classification method for dimensionality reduction adapted to hyperspectral images', *Journal of Applied Remote Sensing*, 11: 025001.

Kumar, Tarun, and Karun Verma. 2010. 'A Theory Based on Conversion of RGB image to Gray image', *International Journal of Computer Applications*, 7: 7-10.

Lorber, Avraham. 1986. 'Error propagation and figures of merit for quantification by solving matrix equations', *Analytical Chemistry*, 58: 1167-72.

MacDonald, Jacqueline, JR Lockwood, John McFee, Thomas Altshuler, and Thomas Broach. 2003. "Alternatives for landmine detection." In.: RAND CORP SANTA MONICA CA.

Makki, Ihab, Rafic Younes, Clovis Francis, Tiziano Bianchi, and Massimo Zucchetti. 2017. 'A survey of landmine detection using hyperspectral imaging', *ISPRS Journal of Photogrammetry and Remote Sensing*, 124: 40-53.

Makki, Ihab, Rafic Younes, Mahdi Khodor, Jihan Khoder, Clovis Francis, Tiziano Bianchi, Patrick Rizk, and Massimo Zucchetti. 2018. "RBF Neural Network for Landmine Detection in H Yperspectral Imaging." In *2018 7th European Workshop on Visual Information Processing (EUVIP)*, 1-6. IEEE.

Manolakis, Dimitris, and Gary Shaw. 2002. 'Detection algorithms for hyperspectral imaging applications', *IEEE signal processing magazine*, 19: 29-43.

Manolakis, Dimitris, Eric Truslow, Michael Pieper, Thomas Cooley, and Michael Brueggeman. 2013. 'Detection algorithms in hyperspectral imaging systems: An overview of practical algorithms', *IEEE signal processing magazine*, 31: 24-33.

Monitor, Landmine, Ban Policy, and Mine Action. 2010. 'Landmine Monitor 2013', *Concord: International Campaign to Ban Landmines*.

Mukhopadhyay, Subhas Chandra, and Gourab Sen Gupta. 2007. *Autonomous Robots and Agents* (Springer).

Ren, Hsuan, Qian Du, Chein-I Chang, and James O Jensen. 2003. "Comparison between constrained energy minimization based approaches for hyperspectral imagery." In *IEEE Workshop on Advances in Techniques for Analysis of Remotely Sensed Data, 2003*, 244-48. IEEE.

Robledo, L, M Carrasco, and D Mery. 2009. 'A survey of land mine detection technology', *International Journal of Remote Sensing*, 30: 2399-410.

Scharf, Louis L, and L Tood McWhorter. 1996. "Adaptive matched subspace detectors and adaptive coherence estimators." In *Conference Record of the Thirtieth Asilomar Conference on Signals, Systems and Computers*, 1114-17. IEEE.

Shibayama, Katsumi. 2009. "Spectrometer." In.: Google Patents.

UNICEF., United Nations. Office of the Special Representative of the Secretary-General for Children, and Armed Conflict. 2009. *Machel study 10-year strategic review: Children and conflict in a changing world* (UNICEF).

Wang, Liguo, and Chunhui Zhao. 2016. *Hyperspectral Image Processing* (Springer).

Wang, Zhou, Alan C Bovik, Hamid R Sheikh, and Eero P Simoncelli. 2004. 'Image quality assessment: from error visibility to structural similarity', *IEEE transactions on image processing*, 13: 600-12.

Yin, Jihao, Yan Wang, Yisong Wang, and Zhanjie Zhao. 2010. "A modified algorithm for multi-target detection in hyperspectral image." In *2010 2nd International Asia Conference on Informatics in Control, Automation and Robotics (CAR 2010)*, 105-08. IEEE.

Yu, Chunyan, Meiping Song, and Chein-I Chang. 2018. 'Band subset selection for hyperspectral image classification', *Remote Sensing*, 10: 113.

Zou, Hui, and Trevor Hastie. 2005. 'Regularization and variable selection via the elastic net', *Journal of the royal statistical society: series B (statistical methodology)*, 67: 301-20.

Zucchetti, Massimo, Mahdi Khodor, Ihab Makki, Rafic Younes, Francis Clovis, and Tiziano Bianchi. 2017. "Landmines. Crisis, legacy, international and local action." In *First International Conference on Landmine: Detection, Clearance and Legislations (LDCL).* 1-6. IEEE.